Electronic Supplementary Information (ESI)

High precision analysis of stable potassium (K) isotopes by the collision cell MC-ICP-MS "Sapphire" and a correction method for concentration mismatch

Xin-Yuan Zheng,[*a] Xin-Yang Chen,[a] Weiming Ding,[a] Yuchi Zhang,[a] Soisiri Charin,[a] and Yvan Gérard[b]

[a]*Department of Earth and Environmental Sciences, University of Minnesota–Twin Cities, Minneapolis, MN 55455, USA. E-mail: zhengxy@umn.edu*

[b]*Nu Instruments, Unit 74 Clywedog Road South Wrexham Industrial Estate, Wrexham LL13 9XS, United Kingdom*
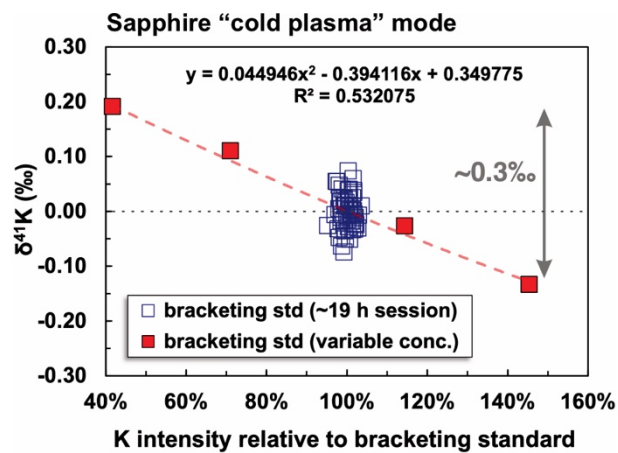
Sapphire "cold plasma" mode

$$y = 0.044946x^2 - 0.394116x + 0.349775$$
$$R^2 = 0.532075$$

Fig. S1 Representative results showing the concentration mismatch effect under "cold plasma" mode on *Sapphire* MC-ICP-MS. All the analyzed solutions came from the same NIST 3141a stock solution but were prepared to have variable K concentrations (red squares). All solutions were analyzed against NIST 3141a. The $\delta^{41}K$ values calculated for each bracketing standard measurement against adjacent bracketing standard measurements were also shown (open squares) and included in the curve fit.
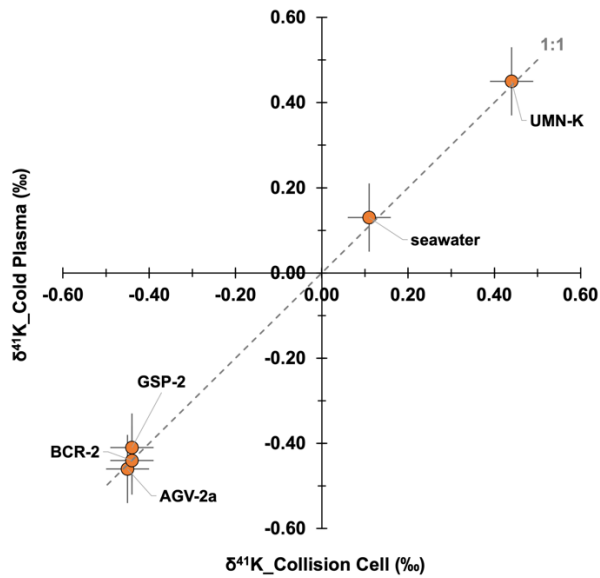
Fig. S2 A comparison of δ^{41}K results measured using the collision cell and "cold plasma" modes of *Sapphire* MC-ICP-MS for 5 different reference materials. Error bars indicate our conservative estimates on precision (2 standard deviations), based on the worst precision obtained from analyses of a suite of reference materials using each method over the course of this study (ESI Table S1).

Table S1. A compilation of δ⁴¹K values for reference materials analyzed in this study

	$\delta^{41}K_{NIST\ 3141a}$ (‰)	2SD[c]	N[d]	Method[e]	Variant	Data Source[f]
Pure K solutions						
NIST 193	0.03	0.02	7	CC		**This study**
	0.02	0.04	2	CP		Hu et al. (2018)
mean	*0.03*	*0.01*				
NIST 918	0.08	0.03	7	CC	NIST 918b	**This study**
	0.08	0.03	4	CP	NIST 918b	Hu et al. (2018)
	0.09[a]	0.22	26*	CP	NIST 918	Morgan et al. (2018)
mean	*0.08*	*0.01*				
NIST 999	0.00	0.02	10	CC	NIST 999c	**This study**
	0.00	0.04	2	CP	NIST 999c	Hu et al. (2018)
	0.09[a]	0.17	55	CP	NIST 999b	Morgan et al. (2018)
	0.02	0.07	28	CP	NIST 999c	Gu et al. (2021)
mean	*0.03*	*0.09*				
UMN-K	0.44	0.05	58	CC		**This study**
	0.45	0.08	32	CP		**This study**
mean	*0.45*	*0.01*				
Geological materials						
GSP	-0.44	0.05	6	CC	GSP-2	**This study**
	-0.41	0.03	2	CP	GSP-2	**This study**
	-0.50	0.11	2	CC	GSP-2	Li et al. (2016)
	-0.36[a]	0.10	3	CP	GSP-2	Morgan et al. (2018)
	-0.45	0.04	2	CP	GSP-2	Li et al. (2020)
	-0.39	0.08	12	CP	GSP-2	Gu et al. (2021)
	-0.41	0.07	5	CP	GSP-2	Huang et al. (2021)
	-0.46	0.09	1	CP	GSP-2	Li et al. (2021a)
	-0.50	0.04	1	CP	GSP-1	Hu et al. (2018)
	-0.44	0.07	1	CP	GSP-1	Chen et al. (2019)
	-0.48	0.06	2	CP	GSP-1	Xu et al. (2019)
	-0.51	0.07	1	CC	GSP-1	Chen et al. (2021)
	-0.51	0.03	2	CC	GSP-1	Moynier et al. (2021b)
mean (GSP-2)	*-0.43*	*0.09*				
mean (GSP-1)	*-0.49*	*0.06*				
mean (all)	*-0.45*	*0.10*				

AGV	-0.45	0.04	8	CC	AGV-2a	**This study**
	-0.46	0.05	3	CP	AGV-2a	**This study**
	-0.47	0.10	2	CC	AGV-2	Li et al. (2016)
	-0.44[a]	0.10	5	CP	AGV-2	Morgan et al. (2018)
	-0.41	0.06	3	CP	AGV-2	Li et al. (2020)
	-0.43	0.10	13	CP	AGV-2	Gu et al. (2021)
	-0.44	0.11	7	CP	AGV-2	Huang et al. (2021)
	-0.49	0.05	9	CP	AGV-2	Liu et al. (2021)
	-0.45	0.03	1	CC	AGV-2	Moynier et al. (2021b)
	-0.45	0.05	1	CP	AGV-1	Hu et al. (2018)
	-0.43	0.11	10	CP	AGV-1	Chen et al. (2019)
	-0.45	0.12	1	CP	AGV-1	Xu et al. (2019)
	-0.42	0.07	1	CP	AGV-1	Hu et al. (2021)
	-0.46	0.08	1	CP	AGV-1	Nie et al. (2021)
	-0.44	0.04	1	CP	AGV-1	Wang et al. (2021b)
	-0.46	0.02	2	CC	AGV-1	Chen et al. (2021)
	-0.45	0.04	1	CC	AGV-1	Moynier et al. (2021b)
mean	*-0.45*	*0.04*				
BCR	-0.44	0.05	27	CC	BCR-2	**This study**
	-0.44	0.04	6	CP	BCR-2	**This study**
	-0.59	0.12	2	CC	BCR-2	Li et al. (2016)
	-0.46	0.12	4	CP	BCR-2	Morgan et al. (2018)
	-0.44	0.11	8*	CP	BCR-2	Jiang et al. (2019)
	-0.46	0.10	11*	CP	BCR-2	Chen et al. (2020)
	-0.38	0.05	3	CP	BCR-2	Li et al. (2020)
	-0.46[a]	0.10	5	CP	BCR-2	Santiago Ramos et al. (2020)
	-0.41	0.05	12	CP	BCR-2	Gu et al. (2021)
	-0.44	0.03	3	CP	BCR-2	Huang et al. (2021)
	-0.55	0.08	1	CP	BCR-2	Liu et al. (2021)
	-0.42	0.06	3	CP	BCR-2	Nie et al. (2021)
	-0.42	0.06	1	CP	BCR-2	Li et al. (2022)
	-0.42	0.09	9	CC	BCR-2	Ku and Jaconsen (2020)
	-0.43	0.03	1	CC	BCR-2	Moynier et al. (2021b)
	-0.42	0.06	1	CP	BCR-1	Hu et al. (2018)
	-0.49	0.06	8	CP	BCR-1	Chen et al. (2019)
	-0.41	0.03	2	CP	BCR-1	Xu et al. (2019)
	-0.41	0.07	4	CP	BCR-1	Huang et al. (2020)
	-0.42	0.06	1	CP	BCR-1	Sun et al. (2020)
	-0.40	0.08	1	CP	BCR-1	Wang et al. (2021b)
	-0.43	0.03	3	CC	BCR-1	Chen et al. (2021)

mean (BCR-2)	*-0.45*	*0.11*				
mean (BCR-1)	*-0.43*	*0.06*				
mean (all)	*-0.44*	*0.09*				
BHVO	-0.42	0.05	10	CC	BHVO-2	**This study**
	-0.50	0.19	1	CC	BHVO-2	Li et al. (2016)
	-0.43[a]	0.24	2	CP	BHVO-2	Morgan et al. (2018)
	-0.46	0.07	13	CP	BHVO-2	Chen et al. (2019)
	-0.41	0.14	13*	CP	BHVO-2	Jiang et al. (2019)
	-0.47	0.06	32*	CP	BHVO-2	Tuller-Ross et al. (2019)
	-0.47	0.10	79*	CP	BHVO-2	Chen et al. (2020)
	-0.40	0.04	2	CP	BHVO-2	Li et al. (2020)
	-0.45	0.07	10	CP	BHVO-2	Li and Han (2021)
	-0.49	0.05	1	CP	BHVO-2	Li et al. (2021a)
	-0.40	0.06	1	CP	BHVO-2	Li et al. (2021b)
	-0.40	0.02	2	CP	BHVO-2	Jiang et al. (2021)
	-0.39	0.08	7	CP	BHVO-2	Nie et al. (2021)
	-0.48	0.10	64*	CP	BHVO-2	Wang et al., (2021a)
	-0.38	0.04	8	CP	BHVO-2	Hobin et al. (2021)
	-0.38	0.09	9	CC	BHVO-2	Ku and Jaconsen (2020)
	-0.48	0.01	4	CC	BHVO-2	Chen et al. (2021)
	-0.38	0.10	8	CP	BHVO-2	Gu et al. (2021)
	-0.52	0.04	2	CP	BHVO-2	Huang et al. (2021)
	-0.37	0.04	1	CC	BHVO-2	Moynier et al. (2021a)
	-0.43	0.04	11	CC	BHVO-2	Moynier et al. (2021b)
	-0.42[b]	0.06	8	CC	BHVO-1	Wang and Jacobson (2016)
	-0.42	0.02	2	CP	BHVO-1	Hu et al. (2018)
	-0.38	0.04	3	CP	BHVO-1	Xu et al. (2019)
	-0.42	0.05	2	CP	BHVO-1	Hu et al. (2020)
	-0.45	0.04	1	CP	BHVO-1	Huang et al. (2020)
	-0.43	0.06	1	CP	BHVO-1	Sun et al. (2020)
	-0.41	0.04	9	CP	BHVO-1	Hobin et al. (2021)
mean (BHVO-2)	*-0.43*	*0.09*				
mean (BHVO-1)	*-0.42*	*0.04*				
mean (all)	*-0.43*	*0.08*				
seawater	0.11	0.05	49	CC		**This study**
	0.13	0.08	6	CP		**This study**
	0.07	0.08	3	CC		Li et al. (2016)
	0.15[b]	0.06	22	CC		Wang and Jacobson (2016)
	0.06	0.10	3	CC		Li et al. (2017)

0.14	0.04	2	CP	Hu et al. (2018)
0.11[a]	0.17	108	CP	Morgan et al. (2018)
0.14	0.01	20	CP	Hille et al. (2019)
0.15	0.04	2	CP	Xu et al. (2019)
0.14	0.07	1	CP	Hu et al. (2020)
0.11	0.06	1	CP	Li et al. (2020)
0.14	0.07	1	CP	Sun et al. (2020)
0.10[a]	0.17	30	CP	Santiago Ramos et al. (2020)
0.14	0.02	4	CP	Teng et al.(2020)
0.11	0.08	46	CP	Wang et al. (2020)
0.11	0.03	4	CC	Chen et al. (2021)
0.13	0.05	2	CC	Moynier et al. (2021b)
0.12	0.07	1	CP	Li et al. (2022)
mean **0.12**	**0.05**			

[a] The data were converted from the reported seawater scale to NIST 3141a scale by adding 0.12‰ (i.e., the reported seawater data were assigned to 0.12‰)

[b] The data were converted from the reported Suprapur scale to NIST 3141a scale by adding 0.05‰, based on Ku and Jacobsen (2019)

[c] When only SE or 95% CI are reported, the uncertainties were converted to SD, SD = SE × $\sqrt{n}$; SD = (95% CI × $\sqrt{n}$) / t, where t is the student t factor, and n is the number of sample-standard bracketing measurements. SD represents intermediate precision for our data, but it may represent repeatability (i.e., repeated measurement of the same solution from the same sample digestion) for some literature data because information on the number of individual digestions for rock reference materials is not always reported in literature.

[d] N is the number of individual replicate analyses; * indicates the number of sample–standard bracketing measurements

[e] CP = cold plasma; CC = collision cell

[f] Full citations are available in the ESI reference section.

Table S2. Apex, *Sapphire*, and data acquisition settings for K isotope analysis

Settings	Collision/reaction cell (LE path)	Cold plasma (HE path)
Apex		
Ar sweep gas flow (L/min)	1.8~2.3	1.3~1.5
N_2 (mL/min)	0	0.2~0.5
Spray chamber temperature (°C)	140	140
Peltier cooler temperature (°C)	3	3
Desolvator temperature (°C)	155	155
Nebulizer gas (L/min)	0.70~0.90	0.70
Nebulizer uptake rate (µL/min)	~100	~100
Sapphire MC-ICP-MS		
Coolant (L/min)	13	13
Aux (L/min)	0.85~1.30	0.80
RF power (W)	1300	700-800
Alpha 1	0	90~100
Alpha 2	0	90~100
Slit position	300-500	1600-1900
Resolving power	~300	10000~12000
Acceleration (V)	~4000	~6000
Extraction (V)	~1820	~3000
RF ref.	0.9~1	–
Cell deceleration	-300.00	–
Cell extraction	-150.00	–
Cell He gas flow (sccm)	2~3	–
Cell H_2 gas flow (sccm)	5~7	–
Data acquisition		
Faraday cup configuration	H6 (10^{11} ohm, ^{41}K), H3 (10^{11} ohm, ^{40}K), L1 (10^{10} ohm, ^{39}K)	H8 (10^{11} ohm, ^{41}K), H2 (10^{11} ohm, ^{39}K)
Integration time (s)	5	5
Number of cycles	50	50
Washout time (s)	120	120
Uptake time (s)	65	65

References

Chen H., Liu X.-M. and Wang K. (2020) Potassium isotope fractionation during chemical weathering of basalts. *Earth and Planetary Science Letters* **539**, 116192, https://doi.org/10.1016/j.epsl.2020.116192.

Chen H., Saunders N. J., Jerram M. and Halliday A. N. (2021) High-precision potassium isotopic measurements by collision cell equipped MC-ICPMS. *Chemical Geology* **578**, 120281, https://doi.org/10.1016/j.chemgeo.2021.120281.

Chen H., Tian Z., Tuller-Ross B., Korotev Randy L. and Wang K. (2019) High-precision potassium isotopic analysis by MC-ICP-MS: an inter-laboratory comparison and refined K atomic weight. *Journal of Analytical Atomic Spectrometry* **34**, 160-171, 10.1039/C8JA00303C.

Gu H.-O. and Sun H. (2021) High-precision analysis of potassium isotopes by MC-ICP-MS without collision cell using cool plasma technique in low-resolution mode. *Journal of Analytical Atomic Spectrometry* **36**, 2545-2552, 10.1039/D1JA00201E.

Hille M., Hu Y., Huang T.-Y. and Teng F.-Z. (2019) Homogeneous and heavy potassium isotopic composition of global oceans. *Science Bulletin* https://doi.org/10.1016/j.scib.2019.09.024.

Hobin K., Costas Rodríguez M. and Vanhaecke F. (2021) Robust Potassium Isotopic Analysis of Geological and Biological Samples via Multicollector ICP-Mass Spectrometry Using the "Extra-High Resolution Mode". *Analytical Chemistry* **93**, 8881-8888, 10.1021/acs.analchem.1c01087.

Hu Y., Teng F.-Z. and Chauvel C. (2021) Potassium isotopic evidence for sedimentary input to the mantle source of Lesser Antilles lavas. *Geochimica et Cosmochimica Acta* **295**, 98-111, https://doi.org/10.1016/j.gca.2020.12.013.

Hu Y., Chen X. Y., Xu Y. K. and Teng F. Z. (2018) High-precision analysis of potassium isotopes by HR-MC-ICPMS. *Chemical Geology* **493**, 100-108, 10.1016/j.chemgeo.2018.05.033.

Hu Y., Teng F.-Z., Plank T. and Chauvel C. (2020) Potassium isotopic heterogeneity in subducting oceanic plates. *Science Advances* **6**, eabb2472, 10.1126/sciadv.abb2472.

Huang C., Gu H.-O., Sun H., Wang F. and Chen B. (2021) High-precision determination of stable potassium and magnesium isotopes utilizing single column separation and multicollector inductively coupled plasma mass spectrometry. *Spectrochimica Acta Part B: Atomic Spectroscopy* **181**, 106232, https://doi.org/10.1016/j.sab.2021.106232.

Huang T.-Y., Teng F.-Z., Rudnick R. L., Chen X.-Y., Hu Y., Liu Y.-S. and Wu F.-Y. (2020) Heterogeneous potassium isotopic composition of the upper continental crust. *Geochimica et Cosmochimica Acta* **278**, 122-136, 10.1016/j.gca.2019.05.022.

Jiang Y., Chen H., Fegley B., Lodders K., Hsu W., Jacobsen S. B. and Wang K. (2019) Implications of K, Cu and Zn isotopes for the formation of tektites. *Geochimica et Cosmochimica Acta* **259**, 170-187, https://doi.org/10.1016/j.gca.2019.06.003.

Jiang Y., Koefoed P., Pravdivtseva O., Chen H., Li C.-H., Huang F., Qin L.-P., Liu J. and Wang K. (2021) Early solar system aqueous activity: K isotope evidence from Allende. *Meteorit Planet Sci* **56**, 61-76, https://doi.org/10.1111/maps.13588.

Ku Y. and Jacobsen S. B. (2020) Potassium isotope anomalies in meteorites inherited from the protosolar molecular cloud. *Science Advances* **6**, eabd0511, doi:10.1126/sciadv.abd0511.

Li W., Beard B. L. and Li S. (2016) Precise measurement of stable potassium isotope ratios using a single focusing collision cell multi-collector ICP-MS. *Journal of Analytical Atomic Spectrometry* **31**, 1023-1029, 10.1039/C5JA00487J.

Li W., Kwon K. D., Li S. and Beard B. L. (2017) Potassium isotope fractionation between K-salts and saturated aqueous solutions at room temperature: Laboratory experiments and theoretical calculations. *Geochimica et Cosmochimica Acta* **214**, 1-13, https://doi.org/10.1016/j.gca.2017.07.037.

Li W., Liu X.-M., Wang K. and Koefoed P. (2021a) Lithium and potassium isotope fractionation during silicate rock dissolution: an experimental approach. *Chemical Geology* **568**, 120142, https://doi.org/10.1016/j.chemgeo.2021.120142.

Li W., Liu X.-M., Hu Y., Teng F.-Z., Hu Y.-F. and Chadwick O. A. (2021b) Potassium isotopic fractionation in a humid and an arid soil–plant system in Hawai'i. *Geoderma* **400**, 115219, https://doi.org/10.1016/j.geoderma.2021.115219.

Li X. and Han G. (2021) One-step chromatographic purification of K, Ca, and Sr from geological samples for high precision stable and radiogenic isotope analysis by MC-ICP-MS. *Journal of Analytical Atomic Spectrometry* **36**, 676-684, 10.1039/D0JA00467G.

Li X., Han G., Zhang Q. and Miao Z. (2020) An optimal separation method for high-precision K isotope analysis by using MC-ICP-MS with a dummy bucket. *Journal of Analytical Atomic Spectrometry* **35**, 1330-1339, 10.1039/D0JA00127A.

Li X., Han G., Liu M., Liu J., Zhang Q. and Qu R. (2022) Potassium and its isotope behaviour during chemical weathering in a tropical catchment affected by evaporite dissolution. *Geochimica et Cosmochimica Acta* **316**, 105-121, https://doi.org/10.1016/j.gca.2021.10.009.

Liu H., Xue Y.-Y., Zhang G., Sun W.-D., Tian Z., Tuller-Ross B. and Wang K. (2021) Potassium isotopic composition of low-temperature altered oceanic crust and its impact on the global K cycle. *Geochimica et Cosmochimica Acta* **311**, 59-73, https://doi.org/10.1016/j.gca.2021.08.001.

Morgan L. E., Santiago Ramos D. P., Davidheiser-Kroll B., Faithfull J., Lloyd N. S., Ellam R. M. and Higgins J. A. (2018) High-precision ^{41}K/^{39}K measurements by MC-ICP-MS indicate terrestrial variability of δ^{41}K. *Journal of Analytical Atomic Spectrometry* **33**, 175-186, 10.1039/C7JA00257B.

Moynier F., Hu Y., Dai W., Kubik E., Mahan B. and Moureau J. (2021a) Potassium isotopic composition of seven widely available biological standards using collision cell (CC)-MC-ICP-MS. *Journal of Analytical Atomic Spectrometry* **36**, 2444-2448, 10.1039/D1JA00294E.

Moynier F., Hu Y., Wang K., Zhao Y., Gérard Y., Deng Z., Moureau J., Li W., Simon J. I. and Teng F.-Z. (2021b) Potassium isotopic composition of various samples using a dual-path collision cell-capable multiple-collector inductively coupled plasma mass spectrometer, Nu instruments Sapphire. *Chemical Geology* **571**, 120144, https://doi.org/10.1016/j.chemgeo.2021.120144.

Nie N. X., Chen X.-Y., Hopp T., Hu J. Y., Zhang Z. J., Teng F.-Z., Shahar A. and Dauphas N. (2021) Imprint of chondrule formation on the K and Rb isotopic compositions of carbonaceous meteorites. *Science Advances* **7**, eabl3929, doi:10.1126/sciadv.abl3929.

Santiago Ramos D. P., Coogan L. A., Murphy J. G. and Higgins J. A. (2020) Low-temperature oceanic crust alteration and the isotopic budgets of potassium and magnesium in

seawater. *Earth and Planetary Science Letters* **541**, 116290, https://doi.org/10.1016/j.epsl.2020.116290.

Sun Y., Teng F.-Z., Hu Y., Chen X.-Y. and Pang K.-N. (2020) Tracing subducted oceanic slabs in the mantle by using potassium isotopes. *Geochimica et Cosmochimica Acta* **278**, 353-360, https://doi.org/10.1016/j.gca.2019.05.013.

Teng F.-Z., Hu Y., Ma J.-L., Wei G.-J. and Rudnick R. L. (2020) Potassium isotope fractionation during continental weathering and implications for global K isotopic balance. *Geochimica et Cosmochimica Acta* **278**, 261-271, https://doi.org/10.1016/j.gca.2020.02.029.

Tuller-Ross B., Savage P. S., Chen H. and Wang K. (2019) Potassium isotope fractionation during magmatic differentiation of basalt to rhyolite. *Chemical Geology* **525**, 37-45, https://doi.org/10.1016/j.chemgeo.2019.07.017.

Wang K. and Jacobsen S. B. (2016) An estimate of the Bulk Silicate Earth potassium isotopic composition based on MC-ICPMS measurements of basalts. *Geochimica et Cosmochimica Acta* **178**, 223-232, http://dx.doi.org/10.1016/j.gca.2015.12.039.

Wang K., Close H. G., Tuller-Ross B. and Chen H. (2020) Global Average Potassium Isotope Composition of Modern Seawater. *ACS Earth and Space Chemistry* **4**, 1010-1017, 10.1021/acsearthspacechem.0c00047.

Wang K., Peucker-Ehrenbrink B., Chen H., Lee H. and Hasenmueller E. A. (2021a) Dissolved potassium isotopic composition of major world rivers. *Geochimica et Cosmochimica Acta* **294**, 145-159, https://doi.org/10.1016/j.gca.2020.11.012.

Wang Z. Z., Teng F. Z., Prelević D., Liu S. A. and Zhao Z. (2021b) Potassium isotope evidence for sediment recycling into the orogenic lithospheric mantle. *Geochemical Perspectives Letters* **18**, 43-47, https://doi.org/10.7185/geochemlet.2123.

Xu Y.-K., Hu Y., Chen X.-Y., Huang T.-Y., Sletten R. S., Zhu D. and Teng F.-Z. (2019) Potassium isotopic compositions of international geological reference materials. *Chemical Geology* **513**, 101-107, 10.1016/j.chemgeo.2019.03.010.